Supporting Information

Title: Resting state functional connectivity of the ventral auditory pathway in musicians with absolute pitch
Authors: Seung-Goo Kim, Thomas R. Knösche
Affiliation: Research Group for MEG and EEG — Cortical Networks and Cognitive Functions Max Planck Institute for Human Cognitive and Brain Sciences, Leipzig, Germany

Corresponding author: Seung-Goo Kim
Postal address: Stephanstraße 1A, 04103 Leipzig, Germany
Phone: +49 341 9940 2618
Facsimile: +49 341 9940 2624
Email: sol@snu.ac.kr

Cross-correlation vs. cross-coherence

Zero-lag cross-correlation quantifies the linear relationship between two time series without time lag. Due to its simplicity, most of the resting-state functional magnetic resonance imaging (rs-fMRI) literature used this measure for functional connectivity (FC). However, cross-correlation and cross-coherence can describe temporal and spectral aspects of coupling of two time series. For a toy example, consider a pair of time series y_1 and y_2 consisting of three components as:

$$y_i = \sum_j \sin\left(w_i f_j \phi_i 2\pi\right),$$

where w is weight, f is frequency, **φ** is phase. The time series y_i is a mixture of the three components. To avoid overlaps between components, frequencies were assigned with prime numbers (i.e., f = 5, 13, or 23 Hz).

Two time series y_1 and y_2 were identical except the second component. By shifting the phase of the second component of the time series y_2, we can systematically change frequency-dependent coupling across two time series. Thus, the phases were varied as **φ** = 0, π/4, π/2, 3π/4, or π. Furthermore, to illustrate the difference between the cross-correlation and cross-coherence, we changed the weight of the second component to 0.5 or 1.5.

In Figure S1, each set of three panels shows waveforms of time series y_1 (red) and y_2 (blue) in the left column, a cross-correlogram in the middle column, and a cross-coherogram in the right column. Zero-lag correlation ("xcor(0)") is noted at the top of the cross-correlogram and cross-coherence for the second component ("xcoh(13)") is noted at the top of the cross-coherogram.

As the phase difference increases, both the zero-lag correlation and the cross-coherence at the second component's frequency (i.e., 13 Hz) decrease. But, it is notable that the decrease rate of the zero-lag correlation is slower than that of the cross-coherence when the weight of the frequency of interest is smaller than other components (Figure S1, A) and vice versa (Figure S1, B). That is, depending on the weight of a specific component that correlates with a regressor of interest, for instance AP group index, we may find a group difference only in the cross-correlation (when the weight is greater) or only in the cross-coherence (when the weight is smaller).

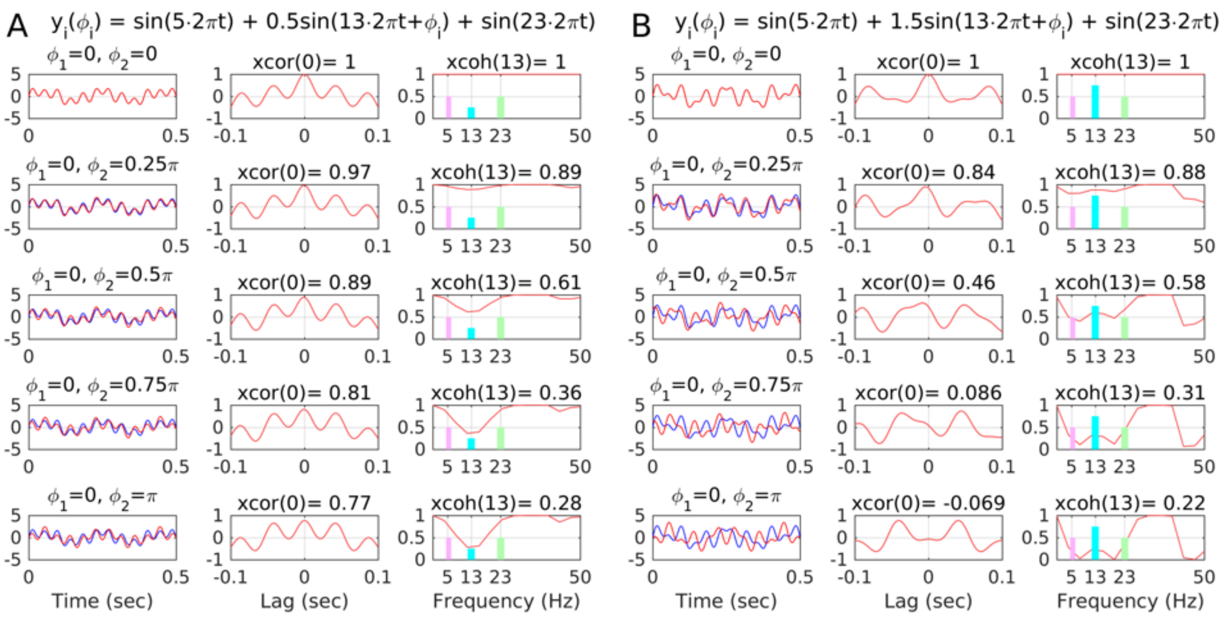

Figure S1. Toy examples on discrepancy between cross-correlation and cross-coherence. In all cases, the reference time series is created with constant phase of zero. For each panel, the weight of the second component (i.e., 13 Hz) is 0.5 (A) and 1.5 (B), respectively. For each row, the phase difference of the second component was 0 to π, and each column within a panel shows two time series (left column), cross-correlation (middle column), and cross-coherence (right column). Zero-lag correlation is noted above the plot for cross-correlation, whereas cross-coherence at the frequency of interest is noted above the plot for cross-coherence. The frequencies of 3 components are marked in the cross-coherence plot by vertical lines (magenta = 5 Hz, cyan = 13 Hz, green = 23 Hz). Abbreviations: xcor, cross-correlation; xcoh, cross-coherence.

Cross-correlation maps

We computed cross-correlation between the time series of the right planum polare (PP) as a seed region and the rest of the cortex over various time-lags between ± 100 s as shown in Figure S2. The magnitude of cross-correlation averaged across wide interval (40 s) was smaller (group averaged correlation between -0.07 and 0.08) compared to the zero-lag cross-correlation (between -0.11 and 0.98). Positive correlations in bilateral superior temporal planes (STPs) and the ventromedial prefrontal cortex (vmPFC), and anterior cingulate cortex (ACC) were shown around the zero-lag, whereas negative correlations in the STPs, vmPFC, and ACC were found in longer lags. The cross-correlation maps were temporally symmetric in general but also showed asymmetry. For instance, the right frontal pole (marked by arrows) showed a positive correlation in negative lags (e.g., -40–0 s) but negative correlation at positive lag (e.g., 0–40 s) unlike STPs that showed a negative correlation in both positive and negative time-lags symmetrically.

Best delay is given a time-lag that maximizes cross-correlation. As already seen in cross-correlation maps, group-averaged best-delay maps (Figure S3) showed temporal asymmetry, for example, the right frontal pole (marked by a black arrow) showed maximal cross-correlation in negative lag, whereas the right superior frontal gyrus (marked by a white arrow) showed maximal correlation in positive lags. Bilateral STPs showed highest correlation in short time-lags and is clearly noticeable from the absolute value of best-delay maps (Figure S4). No effect of AP or APS was found from the non-zero cross-correlation maps or best-delay maps.

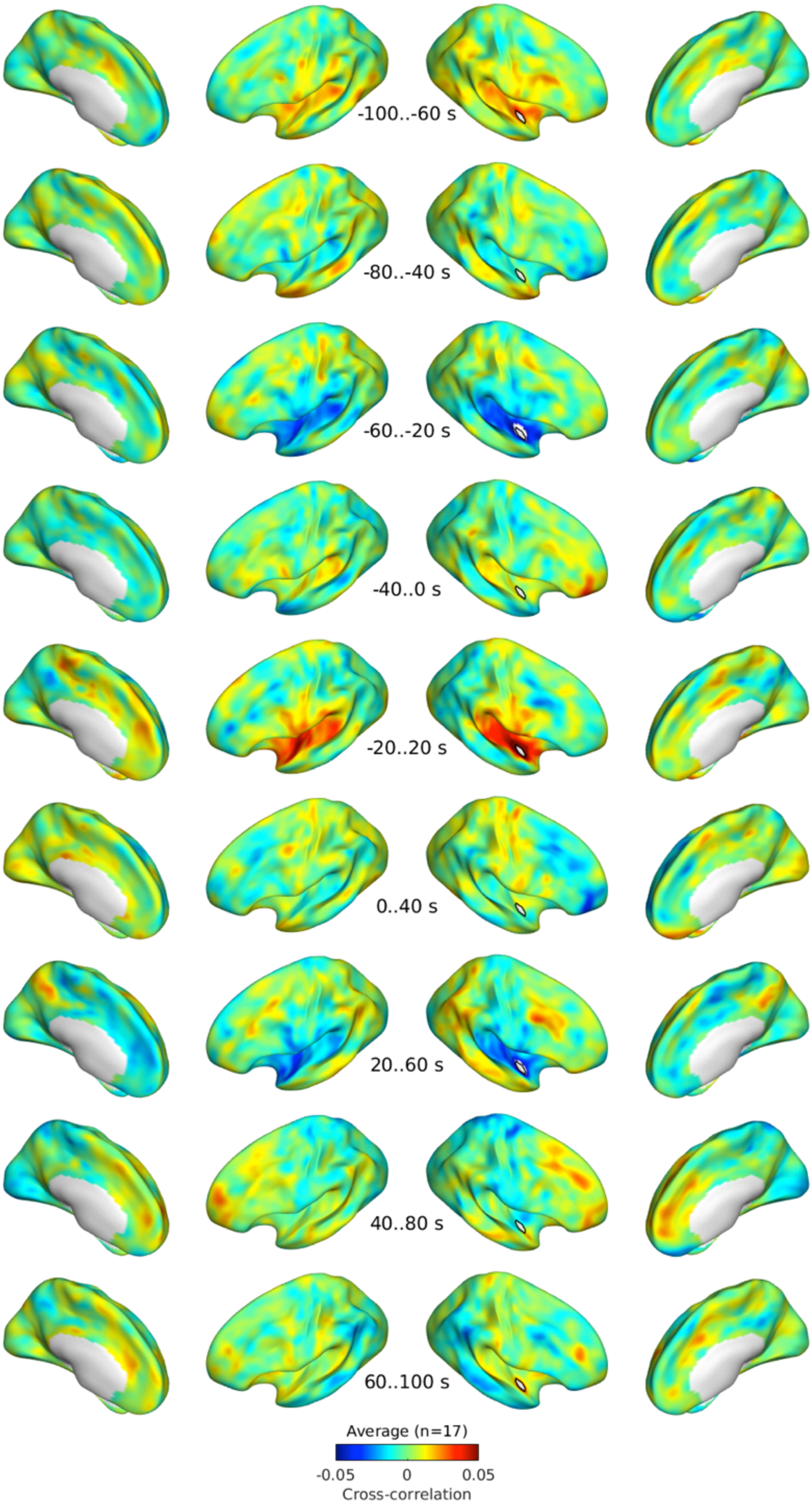
-100..-60 s
-80..-40 s
-60..-20 s
-40..0 s
-20..20 s
0..40 s
20..60 s
40..80 s
60..100 s
Average (n=17)
-0.05
0
0.05
Cross-correlation

Figure S2. Averaged (n = 17) cross-correlation over various time-lag between ± 100 s projected onto semi-inflated cortical surfaces from negative lag (top) to positive lag (bottom).

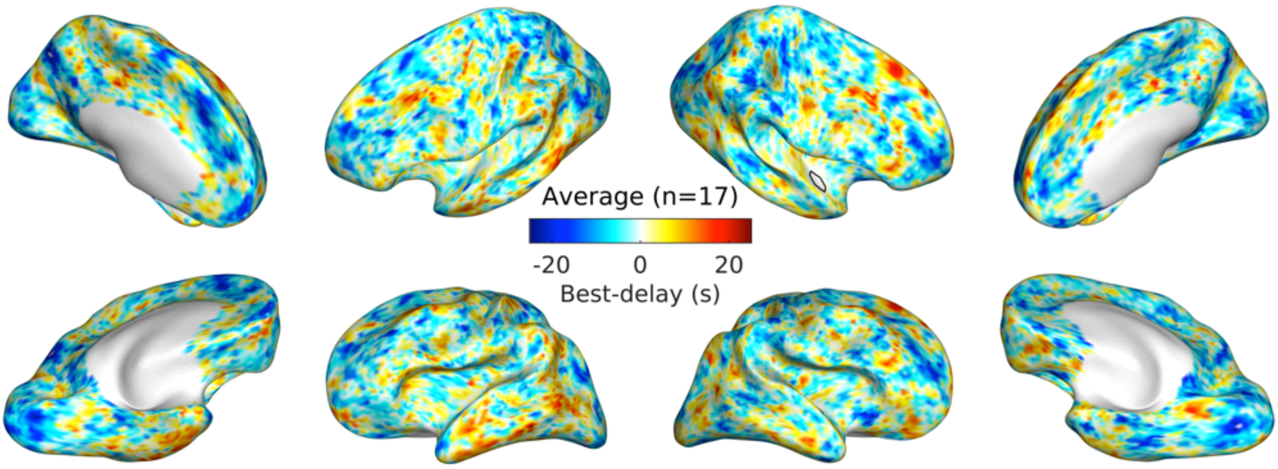

Figure S3. Best delay averaged over all subjects (n = 17) mapped on semi-inflated cortical surfaces.

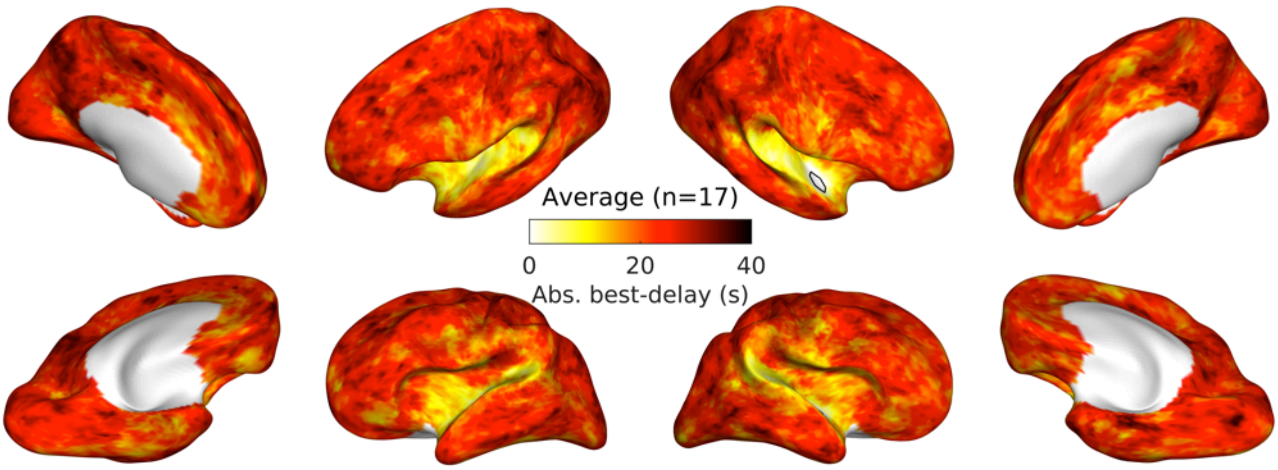

Figure S4. Absolute best delay averaged over all subjects (n = 17) mapped on semi-inflated cortical surfaces.

Cross-coherence maps

Averaged cross-coherence maps across all musicians for all the frequency bins are given in Figure S5. For a 50% overlap between adjacent frequency bins, the cross-coherence maps were similar but consistently showed high coherence on bilateral STPs and gradually smaller overall magnitudes in higher than lower frequency bins.

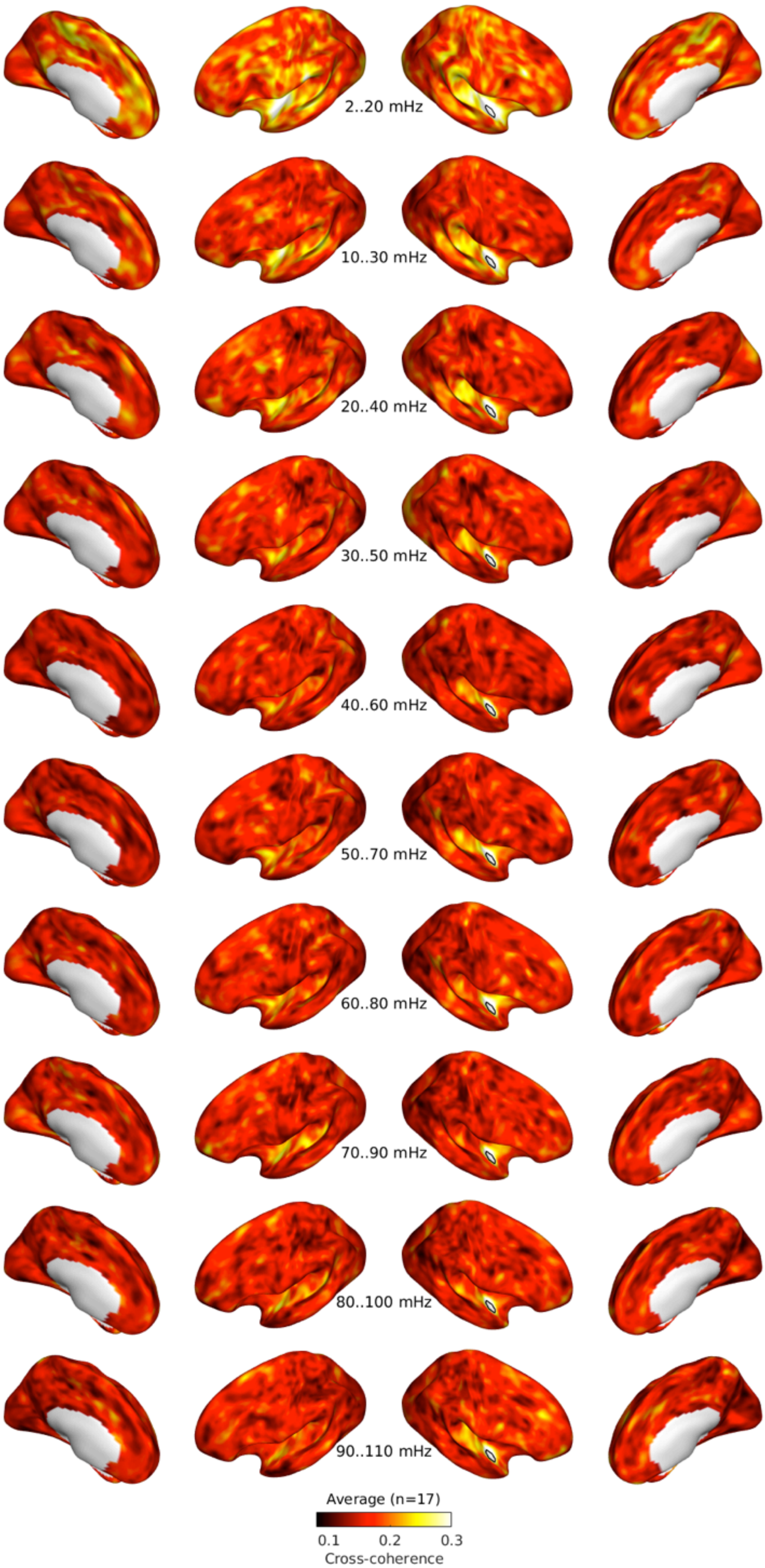
2..20 mHz
10..30 mHz
20..40 mHz
30..50 mHz
40..60 mHz
50..70 mHz
60..80 mHz
70..90 mHz
80..100 mHz
90..110 mHz
Average (n=17)
0.1
0.2
0.3
Cross-coherence

Figure S5. Averaged (n = 17) cross-coherence over multiple frequency bins between 2 and 110 mHz.

Replication only with European musicians

Because the current dataset includes ethnic diversity, its generalization might be limited. To demonstrate that the present findings are not due to the confounding effect of ethnicity, we tested GLMs again only with European but without Asian musicians for RSFC measures that showed significant effects in the main text (i.e., zero-lag cross-correlation and cross-coherence).

With European musicians only, we did not find a significant group difference (min p = 0.195) but found significant effect of APS in zero-lag cross-correlation in the right anterior insula (ICSI-R) and left inferior frontal gyrus (TIFG-L) as in Figure S6.

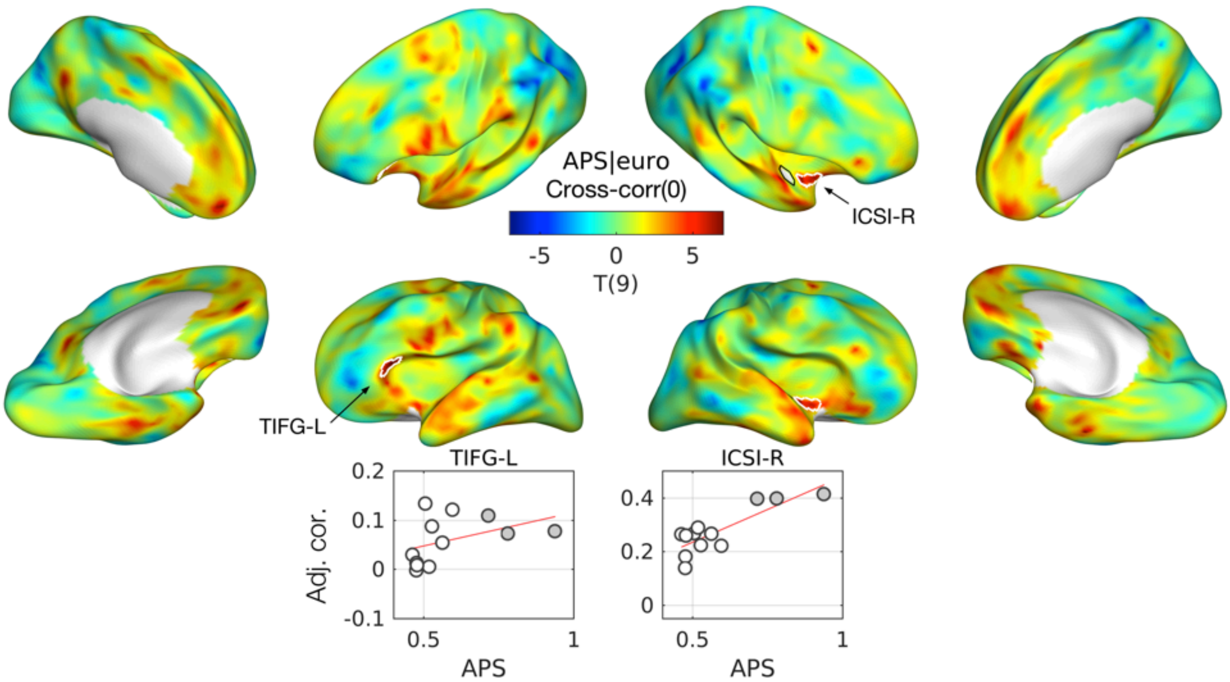

Figure S6. Effect of APS in zero-lag cross-correlation only with European musicians. T-statistic maps are projected onto semi-inflated cortical surfaces. Significant clusters are indicated by white contours. Below the T-maps, scatterplots with regression lines are given for the peak of each cluster. An open circle represents a musician without AP and a gray circle represents a musician with AP. Abbreviations: TIFG-L, triangular part of the left inferior frontal gyrus; ICSI-R, inferior segment of the circular sulcus of the right insula.

We also found a significant effect of AP in cross-coherence between 2 and 40 mHz but found no effect of APS in coherence as in Figure S7. As with the GLM analyses in the main text, the adjacent auditory cortex (FTS/LSTG-R), the contralateral homologous auditory cortex (PP/LSTG-L), ventral auditory cortex (STS-L), and anterior cingulate cortex (ACC-L) were found to be different between the musicians with and without AP. Additionally, the inferior temporal structure (ITG-R) was found to be different between groups as in the analysis with all musicians.

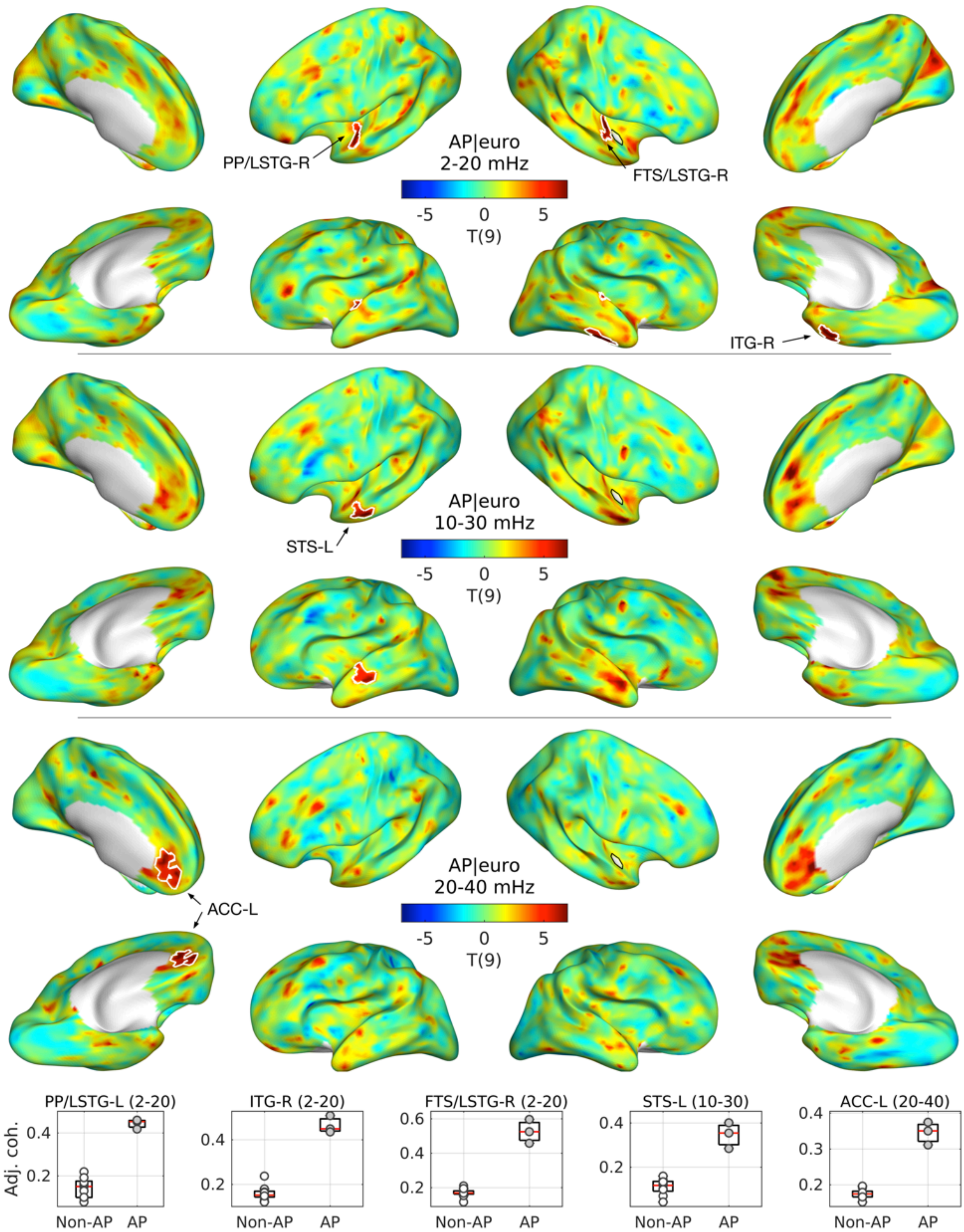

Figure S7. Effect of AP in cross-coherence only with European musicians. T-statistic maps are projected onto semi-inflated cortical surfaces. Significant clusters are indicated by white contours. Below the T-maps, boxplots with regression lines are given for the peak of each cluster. An open circle represents a musician without AP and a gray circle represents a musician with AP. Abbreviations: PP/LSTG-L, left planum polare and lateral superior temporal gyrus; ITG-R, right inferior temporal gyrus; FTS/LSTG-R, right first transverse sulcus and lateral aspect of the left superior temporal gyrus; STS-L, left superior temporal sulcus; ACC-L/R, left/right anterior cingulate cortex.

It is true that not all clusters were found from the GLM only with European musicians. However, because of the relationship between sample size and statistical power, it is not surprising that the GLM result with a subset detects less than one with a full dataset. While the discrepancy between the datasets could be either false positives or false negatives, the cortical regions related to the ventral auditory pathway (i.e., FTS/LSTG-R, PP/LSTG-L, ICSI-R, STS-L) were reliably found in both analyses as well as other cortices such as ACC-L, TIFG-L, of which the implication was discussed in the main text. Moreover, the similarities between the T-maps were very high (Pearson's correlation between 0.96 and 0.98). Therefore, although it was not possible to completely rule out the possibility of the confounding effect from ethnicity, given the evidence of the additional analyses here, we believe the confounding effect is reasonably controlled.